

Synthesis of Ag nanoparticles decorated CeO₂ nanocomposite material for effective SERS analysis

E. Murugan*, S.Santhosh Kumar and A.Raman

Department of Physical Chemistry, School of Chemical Sciences, University of Madras, Chennai 600 025, Tamilnadu, India

*Corresponding author

DOI: 10.5185/amp.2018/870

www.vbripress.com/amp

Abstract

New efficient surface enhanced raman scattering (SERS) nanocomposite material namely silver nanoparticles (AgNPs) decorated Cerium Oxide (AgNPs@CeO₂) was synthesized by adopting simple citrate reduced, precipitation and deposition methods. The synthesized AgNPs@CeO₂ material was characterized with UV-DRS, FTIR, Raman, FESEM, EDX and HRTEM analyses. The obtained results reveal the formation of AgNPs@CeO₂ nanocomposite material with high purity. The FESEM image result confirms that the Ag NPs are decorated on the surface of CeO₂. This AgNPs@CeO₂ nanocomposite was used for fabrication of SERS substrate by drop casted on glass slide. Similarly, for comparative purpose, the pure AgNPs and CeO₂NPs were also fabricated individually on glass slide. The SERS properties for newly fabricated AgNPS@CeO₂, AgNPs and CeO₂ NPs substrate were examined by employed in to detection of 4-aminothiophenol (4-ATP) as a model Raman reporter molecule/analyte. The newly designed AgNPs@CeO₂ material showed excellent SERS properties and sensitivity than that of AgNPs and CeO₂NPs substrates. The enhanced SERS properties noticed in AgNPs@CeO₂ are due to the charge transfer, electromagnetic effect and more hot spots present in metal on metal oxide surfaces. Therefore, it is suggested that the AgNPs@CeO₂ composite material with excellent SERS properties will have an intensive scope for detection of medically significant single analyte/molecule and hence study in that direction are continuing. Copyright © 2018 VBRI Press.

Keywords: AgNPs@CeO₂, hot spot, charge transfer effect, electromagnetic effect, SERS, 4-ATP.

Introduction

Preparation of materials with intensive Surface enhanced Raman scattering (SERS) properties has been widely studied and demonstrated for the application to detection of ultrasensitive chemicals, drug, explosive and biological molecules. Because, the SERS material has a capability for providing molecular fingerprint and rapid pre-treatment on analytes adsorbed on SERS active substrates [1-4]. It is also known from the literature studies that the SERS on rough metal substrates, especially on Ag, Au, and Cu has provides a powerful means for obtaining sensitive frequency resolved vibrational information, related to adsorbate-surface interactions, from high intensity scattering. It is necessary to mention here that the intensive SERS property for any material usually got affected by both electromagnetic enhancement and chemical enhancement effects. Hence, materials with intensive SERS signal are enable to facilitate for effective detection of trace quantity (or) even single molecule through Raman studies. In other words, the chemical enhancement arises through electronic resonance and charge transfer, between a molecule and a

metal surface, resulting in an increase in molecular polarizability. Electromagnetic enhancement, which is usually stronger, takes place under conditions of surface plasmon excitation. The effect of an electromagnetic field is greatly enhanced by amplification of both the incident laser field and the scattered Raman field through surface interactions. Over the past few decades metal on metal oxide systems have received considerable attention because of their extreme importance in both fundamental research and technological applications, for instance, in gas sensors, electronics devices and catalysts [5-8]. Noble metal nanoparticles (Ag, Au, Cu, Ru, Pt, Pd and Cu) have been a focus for intensive research in recent years due to their unique properties which includes chemical, mechanical, electrical and optical characteristics as well as catalytic & biological activities. The poession of their properties in noble metals make them be suitable materials for potential applications in various fields. Among them, AgNPs are particularly attractive because of the relatively low cost and distinctive properties such as superior conductivity, chemical stability, antimicrobial, catalytic activity and SPR sensing [9-12]. This Ag NPs have strong absorption in visible region due to their

unique surface plasmon resonance (SPR), so that they are widely used as SERS analysis events. However, poor chemical and structural stability has been a serious issue, limiting the further practical applications, because the Ag nanostructures tend to evolve into spherical particles, which results in the SPR band blue shift, under various conditions like acids, halides, oxidants, and heat [13-16]. Therefore, development of new experimental strategies for production of stable AgNPs having excellent plasmonic properties and thereby SERS property are highly necessary and leads to studied extensively. It is observed recently that metal oxide/noble metal nanocomposites have shown properties stronger Raman enhancement properties and that is due to the association of localized surface plasmon resonance (LSPR) of the metallic nanoparticles, and charge transfer (CT) effect at the metal oxide/metal interface. The combination of metal oxide (MOx) with metal nanoparticles (MNPs) gives rise to unique synergic properties. That is, the MOx support has effectively stabilized the MNPs through dispersion, controls the activity of NPs due to the interactions with supported MOx. Up to now, several semiconductors, such as metal oxides (TiO₂, ZnO, MoO₃, V₂O₅, SiO₂, CeO₂) have been tested for the SERS properties with noble metal nanoparticles [17-21]. Cerium oxide (CeO₂), a typical kind of multifunctional rare earth oxides, it has been widely investigated because of its multiple applications in chemical-mechanical polishing, UV blockers, catalysts, fuel cells, water treatment, luminescent materials, as an insulating layer on silicon substrates & material with high refractive index and so on. Cerium Oxide nanoparticles have previously been synthesized using a variety of methods including room temperature hydrothermal crystallization, microemulsion, sonochemical synthesis, sol-gel method, spray pyrolysis, solution precipitation, and solvothermal synthesis [22-29]. Among all these methods, solution precipitation method is proved to be ease and environmentally friendly one. It is known from the literature that AgNPs supported CeO₂ material has been prepared bluntly and used in solid-oxide fuel cells, as an electric contact materials and catalyst in various reduction and oxidative reactions. Taking in to consideration of all these facts in this study, it is attempted for fabrication of new SERS material by combining the surface plasmon resonance effect present in AgNPs and charge transfer effect available in CeO₂. Nevertheless, the study on the SERS activity of CeO₂ nanostructures is rarely reported. For the first time, a new efficient surface enhanced raman scattering (SERS) nanocomposite material namely silver nanoparticles decorated Cerium Oxide (AgNPs@CeO₂) was synthesized by adopting the simple citrate reduced, precipitation and deposition methods. The enhancement of SERS properties in newly designed AgNPs decorated CeO₂ nanocomposite was demonstrated in detection of 4-aminothiophenol as a model Raman reporter molecule. The comparative study was also performed and highlighted the achievements of intensive SERS property in the AgNPs@CeO₂.

Experimental

Materials

Silver nitrate (AgNO₃. 99.99 %), Ammonia water solution (NH₃.H₂O. 25%), Sodium citrate Tribasic Dihydrate (TSC) (C₆H₅Na₃O₇.2H₂O. 99%) were purchased from Sisco Research Laboratories Pvt.Ltd., (SRL) with Analytical Reagent (AR) grade. Ammonium Cerium (IV) nitrate ((NH₄)₂ [Ce (NO₃)₆] 99% with ACS grade, purchased from Merck Chemicals. 4-Aminothiophenol (4-ATP, 97 %) purchased from Alfa-aesar. All chemicals were used without further purification. Ethanol (Changshu Yangyuan Chemicals China AR grade 99.99 %) was used as solvent for experiment and sample preparations. All glassware used were thoroughly cleaned with freshly prepared aqua regia (HNO₃/HCl, 1:3, v/v) followed by washing with double-distilled (DD) water and acetone for drying use.

Methods

Synthesis of Silver Nanoparticles (Ag NPs)

The AgNPs were prepared via reduction of AgNO₃ with trisodium citrate, based on the modified method reported by Lee and Meisel [30]. Briefly, 100 mL of a AgNO₃ (1 mM) aqueous solution was heated to 95°C and then a 10 mL aliquot of TSC (1%) solution was added slowly drop by drop. Colour of the solution turns to yellow first and then dark grey colour was obtained. The appearance of color was indicated the formation of silver nanoparticles. The mixture was kept in constant temperature for about 1 hour for get stable nanoparticle and the resultant colloidal mixture was cooled under ambient conditions for characterization and further use.

Synthesis of CeO₂ nanoparticles

The CeO₂ nanoparticles were synthesized by a precipitation method a synthesis method was adopted from previously reported [31]. In a typical synthesis of CeO₂ nanoparticles, first 25 mL of a (NH₄)₂ Ce (NO₃)₆ (0.1 mol/L) solution was stirred vigorously at room temperature for half an hour to ensure complete dissolution. 125 mL of 1.0 mol/L NH₃ (25%) solution was added drop wise into cerium (IV) hydroxide solution. The addition of NH₃ was continued until the pH attained a value of 10 to ensure that all cerium nitrates had been precipitated as cerium hydroxide (Ce(OH)₄) which exist in white color. This precipitate was collected by after centrifugation at 4000 rpm and then washed with water and ethanol several times. The as prepared samples were then dehydrated at 80–120 °C for about 6 h in an oven. Finally, a light yellow CeO₂ powder was obtained. The CeO₂ nanoparticles were calcined in muffle furnaces at temperature 500 °C for 3 h at the rate 3°C/ min and then stored for further use. Double distilled water was used to prepare the solutions.

Preparation of AgNPs@ CeO₂ by Decoration of AgNPs on CeO₂ nanoparticles

CeO₂ having 50 mg was added in to 5 mL of freshly prepared AgNPs solution. It was then sonicated for 15 min and thus observed homogenous mixture. Then the mixture was stirred at 50°C for 4h. Then the obtained mixture was centrifuged at 4000 rpm to remove the undecorated AgNPs by discarded supernatant solution. Then the sample was dried in oven at 60°C for 1h and then it was calcined at 500°C in the rate of 3°C / min. It was stored in desiccator for further studies and characterizations.

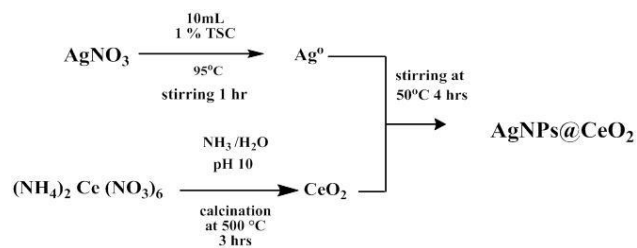
Characterizations

UV spectra were recorded on Perkin Elmer Lambda-35 UV spectrophotometer with analyst software. The measurements were carried out between the wavelength range 200 - 800 nm. FTIR Spectra of CeO₂ and AgNPs@CeO₂ were recorded on Perkin Elmer C 9999 spectrophotometer with analyst software. The measurements were carried out between the wavelength range 400 to 4000 cm⁻¹ conventional method using a thin KBr pellet. High Resolution Transmission electron microscope (JEOL, JEM-1011; Japan) was used to determine the size, shape and the size distribution of the Ag NPs and Ag NPs@ CeO₂ nanocomposite. The surface morphology study was performed using (HITACHI S-3400N) Field Emission scanning electron microscope. The samples were spread on the surface of double sided adhesive carbon tape, one side of which was already adhered to surface of a circular copper disc pivoted by a rod. The samples are dispersed in ethanol and coated on the aluminum foil and then pasted on the carbon tape. Samples were prepared by placing a drop of working solution on a carbon-coated standard copper grid (300 mesh) operating at 80 kV. The SERS spectra of 4-aminothiophenol were recorded with a Confocal Raman spectroscopy (Raman I-11 Model, manufactured by Nano photon Corporation, Japan). The wavelength of laser is 532 nm, uses Neon Argon Laser as the source, laser power - 20 mW. All the measurements were carried out between the range 0 to 3000 cm⁻¹ at 25 °C.

SERS Study

All microscope glass slides (1.5 x 1.5 cm) were cleaned by sonication in water, ethanol each for 2 min successively. Then these substrates were immersed in fresh Piranha solution (4:1 H₂SO₄:30% H₂O₂) (v/v) at 80°C for 30 min to eliminate organic contamination and derive a hydroxyl surface. After cooling, the slides were rinsed repeatedly with DD water and dried. AgNPs@CeO₂ nanocomposite was dispersed 1 min in ethanol by sonication. Then the sample was drop casted on glass slide and dried in room temperature. Raman probe molecule 1x10⁻³ M 4-aminothiophenol (4-ATP) was prepared using ethanol as solvent. 4-ATP was added to AgNPs@CeO₂ nanocomposite and it was washed in ethanol after 30 min then the substrate used for Raman measurements. The above said methods are followed

for the sampling of Ag NPs, CeO₂ and 4-ATP measurements.



Scheme.1. Synthesis of AgNPs@CeO₂ nanocomposite.

Results and discussion

UV-DRS and FTIR Analyses

The SERS substrate namely AgNPs, CeO₂ and newly designed AgNPs@CeO₂ were first examined by UV-DRS, FTIR, HRTEM, FESEM and EDX techniques. The optical (Fig. 1.a) absorption (UV) spectral measurement derived from AgNPs material using UV-visible clearly showed the SPR peak at ~438 nm thus indicates the formation of AgNPs. From the UVDRS spectrum (Fig. 1.b) it is observed that CeO₂ particles give stronger absorbance at 385 nm which support the formation of CeO₂ NPs. In contrast, the UV-DRS spectrum of AgNPs@CeO₂ (Fig.1.b) shows the enhancement of absorbance to 406 nm. The FTIR spectrum of CeO₂ (Fig. 1.c) shows very intense band at 1610 cm⁻¹ which attributed to Ce–O bonds. Supplementary peaks were also observed at 1172, 1050.29, 1108.65 and 975.56 cm⁻¹ and these peaks are corresponds to CeO₂. The stretching frequency of Ce-O observed at ~426.48 cm⁻¹ is agreed were with the previously reported work [32] ie, similarly, the FTIR of AgNPs-CeO₂ shows the characteristic peak at 1050.29 cm⁻¹ which support the formation AgNPs-CeO₂.

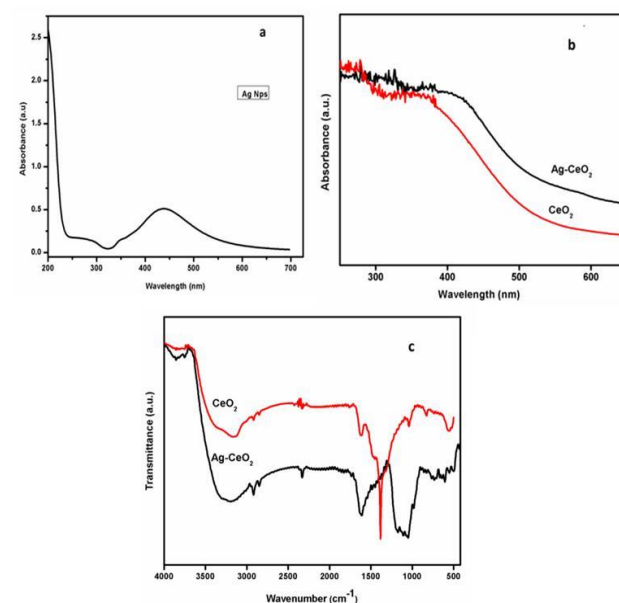


Fig. 1. (a) UV spectra of AgNPs (b) UV-DRS spectrum of CeO₂ and AgNPs-CeO₂ (c) FTIR spectra of CeO₂ and AgNPs-CeO₂.

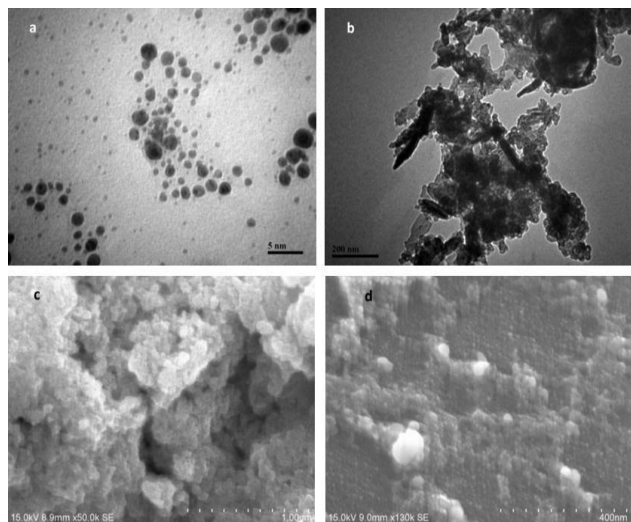


Fig. 2. HRTEM images of a) AgNPs b) AgNPs@CeO₂ and FESEM images of c) CeO₂ d) AgNPs@CeO₂

HRTEM and FESEM analyses

The HRTEM images of the AgNPs and AgNPs@CeO₂ are shown in **Fig. 2.a** and **2.b** respectively. From the HRTEM image of the **Fig. 2.a**, it is observed that AgNPs are exist in several sizes with average diameter of 9 nm and the **Fig. 2.b** proves that the AgNPs decorated on the surface of CeO₂ NPs. The morphology and surface structure of the CeO₂ and Ag NPs@CeO₂ were recorded through FESEM and the obtained images of CeO₂ and AgNPs@CeO₂ were shown in **Fig. 2.c** and **2.d** respectively with different resolutions. From the image **Fig. 2.c**, it is noticed that nanospheres with various sizes were formed and appearance of these spheres supports that the CeO₂ are exist as nano sized particles. Similarly, the image of AgNPs@CeO₂ (**Fig. 2.d**) is shows that intensive tiny dots are available on the surface of nanosize spheres. The tiny dots are due to formation of AgNPs and that in turn decorated onto the surface of nanosized CeO₂ particles.

The EDX analysis is one of the most effective surface characterization technique for identification and semiquantification of surface elements available in AgNPs@CeO₂ composite material and also in control material like viz., CeO₂. The atomic weight percentage of elements present in CeO₂ and AgNPs@CeO₂ was determined with EDX and their obtained spectra were shown in **Fig. 3.a** and **Fig. 3.b** respectively. From **Fig.3.a**, it is noticed that Ce and O are available with 0.30% and 99.70 % respectively. From **Fig. 3.b**, it is observed that Ag (0.99%), Ce (17.64%) and O (77.25%) are available in the AgNPs@CeO₂ composites material. The availability of these elements has strongly confirms the formation of AgNPs@CeO₂ composite materials.

SERS measurements

In order to investigate the SERS activity of newly designed AgNPs@CeO₂ nanocomposite, 4-ATP was

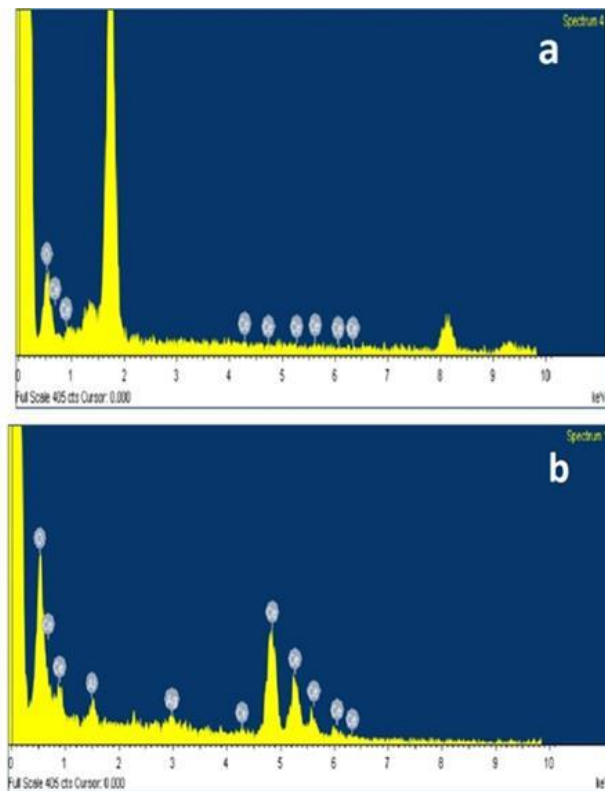


Fig. 3. Elemental analysis of (a) CeO₂ and (b) AgNPs@CeO₂

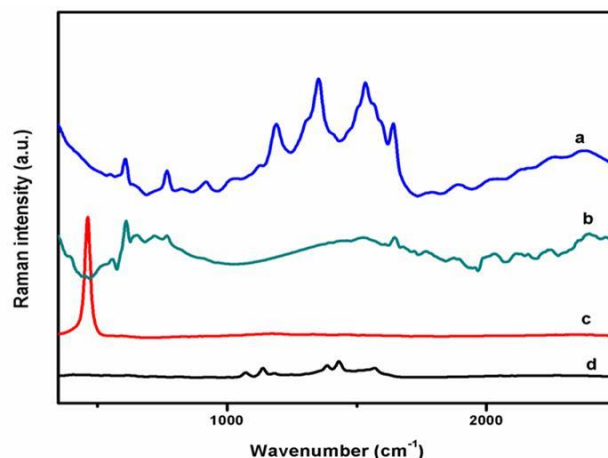


Fig. 4. SERS analysis of 1×10^{-3} M 4-ATP adsorbed on the surface of (a) AgNPs@CeO₂ (b) AgNPs (c) CeO₂ and normal Raman spectrum of (d) 4-ATP.

chosen as a Raman reporter molecule. 4-ATP is an ideal molecule for SERS analysis because it can easily binds to the SERS substrate through Ag-S bond and produced the strong SERS signal, and it also has well-defined Raman vibrational signatures which are essential parameters to ascertain SERS enhancement mechanism. Evaluation of SERS properties for AgNPs, CeO₂ and AgNPs@CeO₂ nanocomposite materials were studied using 4-ATP as a model molecule. **Fig. 4** displays the SERS spectra derived from individual CeO₂, AgNPs and AgNPs@CeO₂ composite materials containing 1×10^{-3} M of 4-ATP. The AgNPs with 4-ATP (**Fig 4.b**) shows clear metal – sulfur (M-S) peak at 1075.41 cm^{-1} . Similarly, the peas for

$[\nu(\text{C-C}) + \delta(\text{C-H})]$ and $\nu(\text{C-C})$ were also noticed at 1390, 1437 and 1567 cm^{-1} respectively while are interpreted as b2 modes. Added to these peaks, a peak at 1014.72 cm^{-1} due to $-\text{SH}$ group of 4-ATP also noticed and this in turn indicates the formation of Ag-S bond. The CeO_2 with 4-ATP spectrum shows that appearance of any peaks related to 4-ATP and hence, it is observed that the 4-ATP has no interaction on the surface of CeO_2 without AgNPs. On combining the SERS spectra for 4-ATP, AgNPs with 4-ATP and Ag@ CeO_2 with 4-ATP, the spectrum obtained from Ag@ CeO_2 with 4-ATP nanocomposite are produced various new peaks with distinct enhancement in band intensity. Especially, the appearance of new peaks at 1014.72, 1191.43, and 1540.03 cm^{-1} were assigned to the $\nu(\text{M-S})$, $\delta(\text{C-H})$, and $\nu(\text{C-C})$ stretching vibration bands respectively, and these bands are dominated with characteristic vibrational modes and these peaks were interpreted as a1 modes. The $[\nu(\text{C-C}) + \delta(\text{C-H})]$ noticed at 1355.87 and 1642.33 cm^{-1} regions, and $\nu(\text{C-C})$ observed at 1540.03 cm^{-1} were interpreted as b2 modes. The band noticed at 606.38 cm^{-1} proves the defect occurred in CeO_2 material and this defect is due to decoration of AgNPs on to the surface of CeO_2 . It is necessary to highlight here that the distinct enhancement of characteristic band intensity 1014.72, 1191.43 and 1540.03 cm^{-1} noticed in AgNPs- CeO_2 4-ATP samples than with their corresponding plain AgNPs 4-ATP, CeO_2 4-ATP and 4-ATP can be explained based on charge transfer and electromagnetic field effects. That is the charge transfer occurred from the CeO_2 support to the Ag particles at the AgNPs- CeO_2 interface inducing a large electromagnetic field. This result suggests that the electrons might migrate from Ag to CeO_2 , thus changing the charge distribution between the two at the interface. Previous studies have reported that the predominance of 4-ATP a1 modes may be attributed to an electromagnetic (EM) enhancement [33, 34]. The intensities of the b2-bands are associated with a charge transfer (CT) mechanism [35]. The Raman spectra suggests both the EM and CT mechanisms contributed to the observed SERS spectra of 4-ATP on the AgNPs@ CeO_2 nanocomposites. It should be noted that on the CeO_2 alone there was no Raman signal, whereas a sharp difference in the Raman spectra between the AgNPs and AgNPs@ CeO_2 was observed. The pure AgNPs creates a weak electromagnetic field that can lead to a weakly enhanced SERS signal for the 4-ATP molecules. On the contrary, we observed a significant much more enhancement was noticed in the case of AgNPs@ CeO_2 nanocomposite over the pure AgNPs. This observation proves that the SERS properties are so weak in the individual Ag or CeO_2 materials, but when they combined together i.e AgNPs@ CeO_2 nanocomposite materials the SERS properties are improved. This can be attributed to a CT transition occurring at the metal-semiconductor interface which induces a strong local electromagnetic field and results in effective Raman enhancement. The predominant enhancement noticed in the band intensity of the characteristic bands is due to the fact that the AgNPs has freely transferring the electrons to the

semiconductor (CeO_2) interface and thus induced the strong localized electromagnetic field. It is thought that the SERS properties of the Ag nanoparticles decorated CeO_2 material arise the formation of defects, such as oxygen vacancies, on the cerium oxide surfaces and uniform SERS "hot spots" after decorating with tiny Ag nanoparticles. Therefore, the occurrence of (i) Charge transfer between AgNPs and CeO_2 (ii) inducement of localized electromagnetic field (iii) Formation of "hotspots" between the AgNPs are synergistically responsible for enhancement of SERS properties observed in AgNPs@ CeO_2 with 4-ATP composite material.

Conclusion

For the first time, stable, cost-effective and efficient SERS material namely AgNPs@ CeO_2 nanocomposite was prepared by adopting the environmentally friendly and simple fabrication (drop casting) method. The enhancement of SERS property in AgNPs@ CeO_2 nanocomposite material was established through UV-DRS, FTIR, HRTEM, FESEM and EDX. However, for practical and real time application, the enhancement of SERS property in AgNPs@ CeO_2 was demonstrated through detection of 4-aminothiophenol as a Raman reporter molecule. The enhanced SERS property noticed in AgNPs@ CeO_2 is due to uniform deposition of AgNPs on the surface of CeO_2 which in turn offering a lot of hot spots. From SERS analysis, it is proved that the combination of AgNPs decorated on cerium oxide has contributed synergetic role for excellent promotion of SERS property. That is, Charge Transfer noticed in CeO_2 and Electromagnetic effect noticed in AgNPs is collectively responsible for enhancement of SERS property. Moreover, the high density of several AgNPs decorated on the surface of CeO_2 nanocomposite provides more "hot spots" on the gaps between neighboring AgNPs and has contributed to considerable or relatively greater Raman signal boost.

Acknowledgements

This work was supported by UGC-UPE-Phase-II New Materials and I acknowledged to NCNSNT for extended the characterization facilities.

References

1. Nie, S. M.; Emory, S. R. *Science*. **1997**, 275, 1102–1106.
DOI: [10.1126/science.275.5303.1102](https://doi.org/10.1126/science.275.5303.1102)
2. Yang, L.; Qin, X.; Jiang, X.; Gong, M.; Yin, D.; Zhang, Y.; Zhao, B. *Phys. Chem. Chem. Phys.* **2015**, 17, 17809.
DOI: [10.1039/c5cp02666k](https://doi.org/10.1039/c5cp02666k)
3. Xu, J.Y.; Wang, J.; Kong, L.T.; Zheng, G.C.; Guoa, Z.; and Liua, J.H. *J. Raman, Spectrosc.* **2011**, 42, 1728–1735.
DOI: [10.1002/jrs.2932](https://doi.org/10.1002/jrs.2932)
4. Silva, W. R.; Keller, E. L.; Frontiera, R. R. *Anal. Chem.* **2014**, 86, 7782–7787.
DOI: [10.1021/ac501701h](https://doi.org/10.1021/ac501701h)
5. Schl'ucker, S. (Ed); Surface Enhanced Raman Spectroscopy; Analytical, Biophysical and Life Science Applications, Wiley: **2011**.
6. Comini, E.; Sberveglieri, G. *Mater. Today*. **2010**, 13, 7-8.
DOI: [10.1016/S1369-7021\(10\)70126-7](https://doi.org/10.1016/S1369-7021(10)70126-7)

7. Ostraat, M.L.; De Blauwe, J.W.; Green, M.L.; Douglas Bell, L.; Atwater, H.A.; Flagan, R.C. *J. Electrochem. Soc.* **2001**, 148(5), G265-G270
DOI: [10.1149/1.1360210](https://doi.org/10.1149/1.1360210)
8. Carnes, C.L.; Klabunde, K.J. *J. Mol. Catal. A: Chem.* **2003**, 194, 227–236.
DOI: [10.1016/S1381-1169\(02\)00525-3](https://doi.org/10.1016/S1381-1169(02)00525-3)
9. Aleksandrova, G. P.; Prozorova, G. F.; Klimenkov, I. V.; Sukhov, B. G.; Trofimov, B. A. *Bull. Russ. Acad. Sci.: Phys.* **2016**, 80, 49–54.
DOI: [10.3103/S1062873816010044](https://doi.org/10.3103/S1062873816010044)
10. Frattini, A.; Pellegrini, N.; Nicastro, D.; de Sanctis, O. *Mater. Chem. Phys.* **2005**, 94, 148.
DOI: [10.1016/j.matchemphys.2005.04.023](https://doi.org/10.1016/j.matchemphys.2005.04.023)
11. Cong, H.; Becker, C.F.; Elliott, S.J.; Grinstaff, M.W.; Porco, J.A. *J. Am. Chem. Soc.* **2010**, 132, 7514–7518.
DOI: [10.1021/ja102482b](https://doi.org/10.1021/ja102482b)
12. Zeng, S.; a Dominique, B.; c Ho-Pui, H.; Yong, K.T. *Chem. Soc. Rev.* **2014**, 43, 3426.
DOI: [10.1039/c3cs60479a](https://doi.org/10.1039/c3cs60479a)
13. Chen, Y.; Wang, C.; Ma, Z.; Su, Z. *Nanotechnology.* **2007**, 18, 325602.
DOI: [10.1088/0957-4484/18/32/325602](https://doi.org/10.1088/0957-4484/18/32/325602)
14. Cathcart, N.; Frank, A.J.; Kitaev, V.; *Chem. Commun.* **2009**, 7170–7172.
DOI: [10.1039/b916902d](https://doi.org/10.1039/b916902d)
15. Zhang, Q.; Ge, J.; Pham, T.; Goebel, J.; Hu, Y.; Lu, Z.; Yin, Y. *Angew. Chem., Int. Ed.* **2009**, 48, 3516–3519.
DOI: [10.1002/anie.200900545](https://doi.org/10.1002/anie.200900545)
16. Jiang, X.C.; Chen, W.M.; Chen, C.Y.; Xiong, S.X.; Yu, A.B. *Nanoscale Resm Lett.* **2011**, 6:32.
DOI: [10.1007/s11671-010-9780-1](https://doi.org/10.1007/s11671-010-9780-1)
17. Xu, S. C.; Zhang, Y. X.; Luo, Y. Y.; Wang, S.; Ding, H. L.; Xu, J. M.; Li, G. H. *Analyst.* **2013**, 138, 4519.
DOI: [10.1039/c3an00750b](https://doi.org/10.1039/c3an00750b)
18. Tao, O.; Li, S.; Ma, C.; Liu, K.; Zhang, Q.Y. *Dalton Trans.* **2015**, 44, 3447.
DOI: [10.1039/c4dt03596h](https://doi.org/10.1039/c4dt03596h)
19. Dong, B.; Huang, Y.; Yu, N.; Fang, Y.; Cao, B.; Li, Y.; Xu, H.; and Sun, M. *Chem. Asian J.* **2010**, 5, 1824 – 1829.
DOI: [10.1002/asia.200900706](https://doi.org/10.1002/asia.200900706)
20. Kong, X.; Yu, Q.; Zhang, X.; Du, X.; Gong, H.; Jiang, H. *J. Mater. Chem.*, **2012**, 22, 7767.
DOI: [10.1039/c2jm16397g](https://doi.org/10.1039/c2jm16397g)
21. Chang, S.; Ruan, S.; Wu, E.; Huang, W. *J. Phys. Chem. C.* **2014**, 118, 19238–19245.
DOI: [10.1021/jp506187d](https://doi.org/10.1021/jp506187d)
22. Yu, S. H.; Colfen, H.; Fischer, A. *Colloid Surf. A.* **2004**, 234, 49–52.
DOI: [10.1016/j.colsurfa.2004.05.006](https://doi.org/10.1016/j.colsurfa.2004.05.006)
23. Kockrick, E.; Schrage, C.; Grigas, A.; Geiger, D.; Kaskel, S. *J. Solid State Chem.* **2008**, 181(7), 1614–1620.
DOI: [10.1016/j.jssc.2008.04.036](https://doi.org/10.1016/j.jssc.2008.04.036)
24. Alamar, T.; Noei, H.; Wang, Y.; Grünert, W.; and Mudring, A.V. *ACS Sustainable Chem. Eng.* **2015**, 3 (1), pp 42–54
DOI: [10.1021/sc500387k](https://doi.org/10.1021/sc500387k)
25. Heb, H.W.; Wub, X.Q; Renb, W.; Shib, P.; Yaob, X.; Songa, Z.T. *Ceram. Int.* **2012**, 38, S501–S504.
DOI: [10.1016/j.ceramint.2011.05.063](https://doi.org/10.1016/j.ceramint.2011.05.063)
26. Elidrissia, B.; Addoua, M.; Regraguia, M.; Montyb, C.; Bougrinea, A.; Kachouanea, A. *Thin Solid Films.* **2000**, 379, 23–27.
DOI: [10.1016/S0040-6090\(00\)01404-8](https://doi.org/10.1016/S0040-6090(00)01404-8)
27. Sreeremya, T. S.; Thulasi, K. M.; Krishnan, A.; Ghosh, S. *Ind. Eng. Chem. Res.* **2015**, 1, 318–326.
DOI: [10.1021/ie2019646](https://doi.org/10.1021/ie2019646)
28. Zhai, Y.; Zhang, S.; Pang, H. *Mater Lett.* **2007**, 61, 1863–1866.
DOI: [10.1016/j.matlet.2006.07.146](https://doi.org/10.1016/j.matlet.2006.07.146)
29. Inoue, M.; Kimura, M.; Inui, T. *Chem. Commun.* **1999**, 11, 957–958.
DOI: [10.1039/A900930B](https://doi.org/10.1039/A900930B)
30. Pouretedal, H. R.; Kadkhodaie, A. *Chin. J. Catal.*, **2010**, 31, 1328–1334.
DOI: [10.1016/S1872-2067\(10\)60121-0](https://doi.org/10.1016/S1872-2067(10)60121-0)
31. Lee, P. C.; Meisel, D. *J. Phys. Chem.* **1982**, 86, 3391–3395.
DOI: [10.1021/j100214a025](https://doi.org/10.1021/j100214a025)
32. Srivastava, M.; Das, A.K.; Khanra, P.; Uddin, E.; Kim, N.H.; Lee, J.H. *J. Mater. Chem. A.* **2013**, 1, 9792.
DOI: [10.1039/C3TA11311F](https://doi.org/10.1039/C3TA11311F)
33. Yang, L.; Jiang, X.; Ruan, W.; Yang, J.; Zhao, B.; Xu, W.; Lombardi, J. R. *J. Phys. Chem. C.* **2009**, 113, 16226–16231.
DOI: [10.1021/jp903600r](https://doi.org/10.1021/jp903600r)
34. Hsieh, C. W.; Lin, P. Y.; Hsieh, S.; *J. Nanophotonics.* **2012**, 6, 063501–063506.
DOI: [10.1117/1.JNP.6.063501](https://doi.org/10.1117/1.JNP.6.063501)
35. Fromm, D. P.; Sundaramurthy, A.; Kinkhabwala, A.; Schuck, P. J.; Kino, G. S.; Moerner, W. E. *J. Chem. Phys.* **2006**, 124, 61101.
DOI: [10.1063/1.2167649](https://doi.org/10.1063/1.2167649)